Generalized survival in step fluctuations

C. G. Tao, W. G. Cullen, and E. D. Williams*
Department of Physics and Materials Research Science and Engineering Center, University of Maryland, College Park, Maryland 20742-4111, USA

C. Dasgupta
Department of Physics, Indian Institute of Science, Bangalore 560012, India
(Received 11 December 2006; published 14 August 2007)

The properties of the generalized survival probability, that is, the probability of not crossing an arbitrary location R during relaxation, have been investigated experimentally (via scanning tunneling microscope observations) and numerically. The results confirm that the generalized survival probability decays exponentially with a time constant $\tau_s(R)$. The distance dependence of the time constant is shown to be $\tau_s(R) = \tau_{s0}\exp[-R/w(T)]$, where $w^2(T)$ is the material-dependent mean-squared width of the step fluctuations. The result reveals the dependence on the physical parameters of the system inherent in the prior prediction of the time constant scaling with R/L^{α}, with L the system size and α the roughness exponent. The survival behavior is also analyzed using a contrasting concept, the generalized inside survival $S_{\text{in}}(t,R)$, which involves fluctuations to an arbitrary location R further from the average. Numerical simulations of the inside survival probability also show an exponential time dependence, and the extracted time constant empirically shows $(R/w)^{\lambda}$ behavior, with λ varying over 0.6 to 0.8 as the sampling conditions are changed. The experimental data show similar behavior, and can be well fit with $\lambda=1.0$ for $T=300$ K, and $0.5<\lambda<1$ for $T=460$ K. Over this temperature range, the ratio of the fixed sampling time to the underlying physical time constant, and thus the true correlation time, increases by a factor of $\sim 10^3$. Preliminary analysis indicates that the scaling effect due to the true correlation time is relevant in the parameter space of the experimental observations.

DOI: 10.1103/PhysRevE.76.021601 PACS number(s): 68.37.Ef, 68.65.−k, 05.20.−y, 05.40.−a

I. INTRODUCTION

The stability of nanometer scale materials and devices is a fundamental and challenging issue [1–5]. A key problem associated with nanoscale stability is random stochastic interface dynamics, which can be directly observed in fluctuations of crystal-layer boundaries (steps) [6–11]. Such fluctuations can be evaluated using correlation function approaches, however, additional information is available by considering first-passage questions [12], such as the temporal persistence probability $P(t)$ and survival probability $S(t)$. Recently, first passage concepts have been applied to a variety of different problems, including ion channels in biology, single molecule electron transfer, etc. [13–16]. In addition, the fluctuations of line boundaries where a surface changes height by one crystalline layer (steps) have previously been used as tests of theoretical predictions for persistence probability and survival probability [17–23]. Here we will address generalizations of the survival concept to include issues of first passage to arbitrary locations. The motivation for addressing this concept is the potential for applications in which nanoscale structures may fluctuate to a point of encounter at which a change in properties or other switching behavior may occur.

The definition of survival probability $S(t)$ is the probability of the step edge not returning to the fixed average step position within a given time interval t. Both theoretical and experimental studies have shown that the survival probability $S(t)$ decays exponentially at large times, $S(t)\sim\exp(-t/\tau_s)$, where τ_s is the survival time constant, which is directly proportional to the correlation time τ_c [24,25]. To generalize this analysis, the return position can be shifted from the average position to an arbitrary reference position R. In this case, the generalized survival probability $S(t,R)$ can be defined as the probability that the step position is initially beyond the pre-assigned reference position R $(-R)$ and remains there (does not relax) over a given time interval t [26], as schematically drawn in Fig. 1. Similar to the survival probability, the generalized survival probability also is predicted to have a long time exponential behavior $S(t,R)\sim\exp[-t/\tau_s(R)]$, where $\tau_s(R)$ is the generalized survival time constant [26]. Herein, our experimental results of step fluctuations on Ag(111) observed by time dependent scanning tunneling microscopy (STM) confirm this prediction, and provide a generalization of the scaling form of the generalized survival that can be used to predict the survival properties of step fluctuations at different temperatures. Furthermore, we introduce a contrasting concept, noted as the generalized inside survival $S_{\text{in}}(t,R)$, the probability of the step position remaining between the pre-assigned reference positions R and $-R$. Correlated experimental and numerical investigation of this concept show distinctly different behavior than for the generalized survival.

II. EXPERIMENTAL AND NUMERICAL PROCEDURES

The experimental process to make Ag films on freshly cleaved mica substrates has been reported previously [27–29]. The thickness of the Ag films used in this work is about 500 nm. After several sputtering and annealing cycles

*Email address: edw@umd.edu

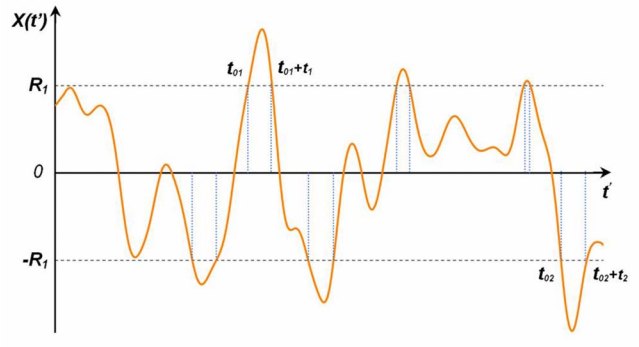

FIG. 1. (Color online) Schematic representation of temporal step wavelengths and the definition of the offset reference position R. Any interval of time over which the step remains $>R_1$ ($<-R_1$) represents a survival event. For instance, in any interval between t_{01} and $t_{01}+t_1$ or between t_{02} and $t_{02}+t_2$ the step trajectory has survived by not crossing R_1 ($-R_1$). The solid orange line indicates the step position. The vertical dashed blue lines indicate time intervals for $S(t,R)$ with respect to the reference position R_1 ($-R_1$).

in a UHV chamber (base pressure $<5\times10^{-10}$ Torr), atomically clean Ag(111) surfaces are obtained, as determined by AES low-energy electron diffraction, and STM. Under proper annealing conditions, the width of flat (111)-oriented terraces can be larger than 1 μm, and step density is quite low, as shown in Fig. 2.

Following cleaning, the samples are transferred to a commercial variable temperature STM (Omicron) in the same UHV chamber, where temperature is controlled with a PBN heater. Step fluctuations are observed in real time by scanning the tip over a fixed position on the step edge in the direction perpendicular to the step orientation. The typical tunneling current is 0.07 to 0.10 nA, and sample bias -1.60 to -1.70 V, chosen to insure that tip-sample interactions do not modify the step fluctuations [6,29,30]. For each temporal pseudoimage, the scan time interval δt between scan lines is 51.2 ms, and the total measurement time t_m is 102.4 s with 2000 lines. The pseudoimages are presented in Fig. 3. Ten to twenty pseudoimages are measured to obtain the data set at each different temperature. The temporal motion of the step edge, the step-edge position $x(t)$, is extracted from each line scan after flattening the upper or lower terrace in the image. The step edge is identified as the point at which the surface height is midway between the heights of the upper and lower terraces. The individual $x(t)$ data sets are used to calculate the distribution of displacements, the temporal correlation, autocorrelation and survival functions, and here the reported functions are averaged over ten to fifteen individual data sets. Measurements were performed in the temperature range from 300 to 460 K by indirectly heating samples using the PBN heater.

FIG. 2. (Color online) STM topography image of an 800×800 nm^2 Ag(111) surface. Tunneling conditions are $U_{\text{sample}}=-1.70$ V and $I_t=95$ pA.

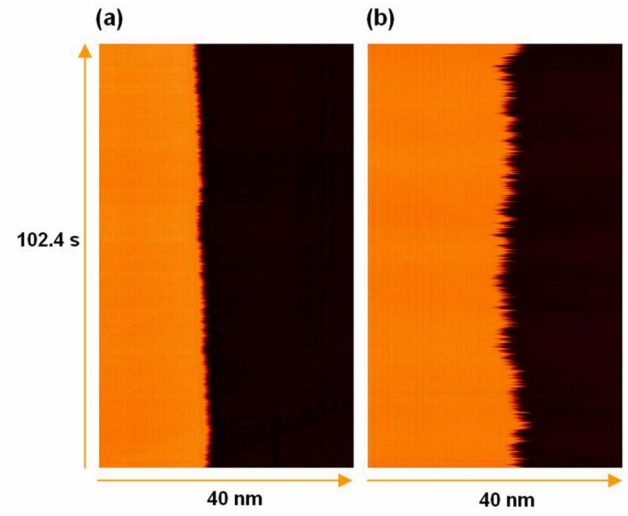

FIG. 3. (Color online) STM temporal pseudoimages obtained by scanning the STM tip over a fixed position on the step edge in the direction perpendicular to the step orientation. For both images, the line-scan length is 40 nm, a line-scan time 51.2 ms, and total time 102.4 s with 2000 lines. The step orientations are along a close-packed direction. The images are obtained at 300 K (a) and at 460 K (b).

We have also studied the behavior of the generalized survival probability $S(t,R)$ and the generalized inside survival probability $S_{\text{in}}(t,R)$ by carrying out numerical integrations of the one dimensional Edwards-Wilkinson (EW) equation (dynamical exponent $n=2$) and the conserved-noise fourth order Langevin equation ($n=4$). Since the experimental observations indicate that the model with $n=4$ is appropriate for the systems studied here (see below), we present herein the results obtained for this model. Simulation results for the generalized inside survival probability for the nonconserved EW equation with $n=2$ will be reported elsewhere [31].

The spatially discretized, dimensionless form of the Langevin equation used in the numerical work is

$$\frac{dx_i}{dt} = -(x_{i-2} - 4x_{i-1} + 6x_i - 4x_{i+1} + x_{i+2}) + \eta_i(t), \qquad (1)$$

where $x_i(t)$ represents the step position at lattice site i at time t, and $\eta_i(t)$ are random variables with zero mean and correlations given by $\langle \eta_i(t)\,\eta_j(t')\rangle = \delta_{t,t'}[2\delta_{i,j} - \delta_{i,j+1} - \delta_{i,j-1}]$. For a

system of L sites with periodic boundary conditions, the equilibrium width is then given by $w^2(L)=L/24$, and the correlation time in the long-time equilibrium state is $\tau_c(L)=(L/2\pi)^4$. The simulations were done for $L=200$; some results were also obtained for $L=100$ and $L=400$. Starting from a straight step profile ($x_i=0$ for all i), the system was equilibrated by carrying out the time integration for a sufficiently long period, and the resulting equilibrated configuration were used as the starting point of further time integration for calculating the generalized survival probabilities. Since the noise is conserved, the average step position $\langle x\rangle \equiv (\Sigma_{i=1}^{L} x_i)/L$ remains equal to zero at all times and there is no need to subtract it from $x_i(t)$ to define the instantaneous step displacement from the average value. The results for the survival probabilities were obtained from averages over 10^4 independent runs.

III. RESULTS AND ANALYSIS

As described in the experimental section, the step-edge position $x(t)$ can be extracted from the measured pseudoimages such as those shown in Fig. 3. Given $x(t)$ we can directly calculate the temporal correlation functions $G(t)$ [7]

$$G(t) = \langle (x(t) - x(0))^2 \rangle = \left(\frac{2\Gamma(1-1/n)}{\pi} \right) \left(\frac{kT}{\tilde{\beta}} \right)^{(n-1)/n} (\Gamma_n t)^{1/n}, \tag{2}$$

where Γ_n is the step mobility and $\tilde{\beta}$ the step stiffness. The simulations [Eq. (1)] are carried out at a fixed value of $\Gamma_n \tilde{\beta}/kT$. Since the step stiffness $\tilde{\beta}$ depends on both temperature and step orientation [32], we measure only steps oriented along the close-packed direction. The measured correlation functions consistently grow as $t^{1/n}$ with $1/n$ close to $1/4$, indicating that the step edge fluctuations are dominated by periphery diffusion in this temperature range, as expected from previous reports [6,29,30]. The pseudoimages in Fig. 3 also clearly reveal a strong increase in fluctuation amplitude with temperature. The average step width $w=\sqrt{\langle [x(t)-\bar{x}]^2 \rangle}$, where $\bar{x}$ the temporal average of the measured step position, is 0.136 ± 0.007 nm at 300 K, and about seven times larger, 0.908 ± 0.043 nm at 460 K. (The stiffness $\tilde{\beta}$ is a decreasing function of temperature.) If the step configuration is equilibrated, the distribution of step displacements $x(t)-\bar{x}$ is expected to be Gaussian with a width equal to the equilibrium step width [33,34]. This is confirmed experimentally, as shown by the distribution of step displacements at 460 K in Fig. 4, which has an equilibrium width 0.930 ± 0.010 nm, the same as the directly calculated step width above.

The survival probability is related to the autocorrelation function [35]

$$C(t) = \langle [x(t_0+t) - \bar{x}][x(t_0) - \bar{x}] \rangle_{t_0} = C(0) \left[(e^{-t/\tau_c}) - \Gamma\left(\frac{3}{4}, \frac{t}{\tau_c} \right) \left(\frac{t}{\tau_c} \right)^{1/4} \right], \tag{3}$$

where τ_c is the correlation time, which is related to the effective system size as $\tau_c = kT(L_{\text{eff}}/2\pi)^n/\Gamma_n\tilde{\beta}$. The first term in Eq. (3) becomes dominant when t is large, so the long time behavior of correlation functions is an exponential decay. The measured autocorrelation function data are well fitted by the form in Eq. (3) [29], and for the data presented here yield correlation times τ_c, equal to 11.8 ± 4.9 s at 300 K and 15.1 ± 5.9 s at 460 K. This is consistent with the previous observation of measurement-time limited correlation time of $\tau_c = t_m/(9\pm4)$ [29]. The measurement time dependence arises from the increase in the time constant for fluctuations of increasing wavelength. Only those wavelengths with time constant substantially less than the measurement time are properly sampled. The longest properly sampled wavelength sets the effective system size and thus the correlation time [29]. Using the relationships between measurement time and correlation time, and correlation time and effective system size, the measured values of the step width therefore depend also on the measurement time

$$w = \sqrt{kTL_{\text{eff}}/12\tilde{\beta}} = (2\pi kT/12\tilde{\beta})^{1/2} (\Gamma_n \tilde{\beta} t_m/AkT)^{1/2n} \tag{4}$$

as well as on the physical parameters of temperature, step stiffness, and step mobility.

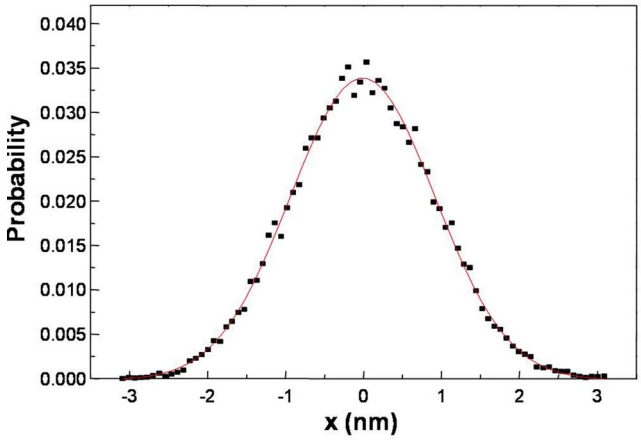

FIG. 4. (Color online) The distribution of step displacements at 460 K. The red fitting curve is Gaussian fit of the data with a width 0.930 ± 0.010 nm.

A. Generalized survival

The $x(t)$ data are also used to determine the generalized survival probability $S(t,R)$, the probability for the step position to remain above (below) a certain preassigned reference position R ($-R$) over a time interval t [26]

$$S(t,R) \equiv \text{Prob}\{[x(t') > R] \vee [x(t') < -R], \quad \forall\, t_0 \leq t' \leq t_0 + t\}. \tag{5}$$

In analyzing the experimental data we chose R values equal to $w/5$, $2w/5$, $3w/5$, $4w/5$, and w. The results are presented in Fig. 5 for the measurement at 460 K. The uppermost curve corresponds to the usual survival probability $S(t)$ with respect to $R=0$, which clearly shows exponential decay in the intermediate time regime. The deviation from exponential

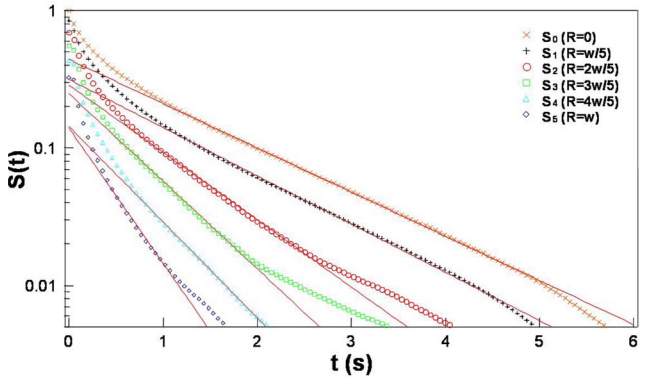

FIG. 5. (Color online) The generalized survival probability curves $S(t,R)$ and corresponding fitting curves at 460 K. From upper to lower, the curves are respectively the generalized survival probability with respect to $R=0$, $w/5$, $2w/5$, $3w/5$, $4w/5$, and w. The solid red lines are corresponding exponential fits for each curve. The time constants extracted from the fits are listed in Table I.

behavior at long times is caused by the limit of the total measurement time, which has been discussed in detail in earlier work [25,29]. The red straight lines are fits of the experimental data to a generalized exponential form $S(t,R) \sim \exp[-t/\tau_s(R)]$. The behavior is consistent with the theoretical prediction that, given an exponential autocorrelation function, the corresponding survival probability should have related exponential behavior [35]. Fitting $S(t,R=0)$ to an exponential form $S(t,R=0) \sim \exp(-t/\tau_s)$ yields the survival time constants τ_s, which are 1.38 ± 0.20 s at 300 K and 1.35 ± 0.10 s at 460 K, approximately 1/10 the magnitude of the correlation time. From upper to lower, the other curves are the generalized survival probability with R increasing from $w/5$ to w. The measured generalized survival probabilities $S(t,R)$ for different R all decay exponentially at intermediate time. As R increases, the generalized survival probability decays faster. This is consistent with numerical simulations of the generalized survival probability that were carried out for a one-dimensional model that provides a discrete realization of the nonconserved EW equation [26].

We confirmed numerically that the generalized survival probability $S(t,R)$ for the fourth-order conserved equation exhibits the same general behavior as that found in simulations [26] of the EW model. In particular, we find that $S(t,R)$ decays exponentially with time at long times, and that the time constant $\tau_s(R)$ of the exponential decay is a decreasing function of the distance R. The dependence of τ_s on R is consistent with the exponential form $\tau_s(R) \propto \exp(C_1 R/w)$, where w is the equilibrium width of the step and C_1 is a constant. It should be noted here that this functional form is purely empirical, and although our results for τ_s are consistent with this form, other forms for the dependence of τ_s on R cannot be ruled out. The observed dependence of $S(t,R)$ on the system size L and the sampling time δt (i.e., the time interval between two successive measurements of the step position in the calculation of the generalized survival probability) is also similar to that found for the EW model [26].

The experimental values of the survival probability at $t=0$, $S(0)$ and the time constants $\tau_s(R)$ extracted from the fits are listed in Table I and the time constants are plotted in Fig. 6(a). The time constants $\tau_s(R)$ decrease exponentially with R, with different length-constants at different temperatures, as shown in Fig. 6(a). When R is normalized by the step width w, the $\tau_s(R/w)$ curves at 300 and 460 K almost collapse on each other as shown in Fig. 6(b). Exponential fits to the

TABLE I. Experimental parameters determined from fits to experimental $x(t)$ data. The root mean-squared width w is determined from the distribution of $x(t)$ as in Fig. 4, the correlation time is determined from fits to Eq. (4). The generalized survival intercepts, e.g., the experimentally measured values at $t=0$ [$S(0)$ and $S_{\text{in}}(0)$] are shown and the time constants (τ_s and τ_{sin}) extracted from the $x(t)$ data using Eqs. (11) and (12). The offset values range from $R=0$ to $R=w$. The known values of the Gaussian integral [Eq. (10)] yield expected values of $S(0)$ that are 1 ($R/w=0$), 0.841 ($R/w=0.2$), 0.689 ($R/w=0.4$), 0.549 ($R/w=0.6$), 0.424 ($R/w=0.8$), and 0.317 ($R/w=1.0$).

T (K)	w (nm) τ_c (s)	R/w	$S(0)$	$\tau_s(R)$	$S_{\text{in}}(0)$	$\tau_{\text{sin}}(R)$
300	$w=0.136 \pm 0.007$	0	1.00	1.38 ± 0.20		
	$\tau_c=11.8 \pm 4.9$	0.2	0.84 ± 0.04	1.09 ± 0.22	0.16 ± 0.04	0.10 ± 0.03
		0.4	0.69 ± 0.06	0.88 ± 0.35	0.31 ± 0.06	0.21 ± 0.05
		0.6	0.54 ± 0.05	0.81 ± 0.10	0.46 ± 0.06	0.29 ± 0.03
		0.8	0.42 ± 0.03	0.61 ± 0.12	0.58 ± 0.03	0.36 ± 0.07
		1.0	0.31 ± 0.03	0.47 ± 0.15	0.69 ± 0.03	0.57 ± 0.05
460	$w=0.908 \pm 0.043$	0	1.00	1.35 ± 0.10		
	$\tau_c=15.1 \pm 5.9$	0.2	0.85 ± 0.01	1.24 ± 0.13	0.15 ± 0.01	0.04 ± 0.01
		0.4	0.69 ± 0.02	0.89 ± 0.10	0.31 ± 0.02	0.08 ± 0.01
		0.6	0.56 ± 0.02	0.68 ± 0.08	0.4 ± 0.022	0.13 ± 0.01
		0.8	0.43 ± 0.02	0.62 ± 0.17	0.57 ± 0.02	0.27 ± 0.02
		1.0	0.32 ± 0.02	0.44 ± 0.11	0.68 ± 0.02	0.44 ± 0.04

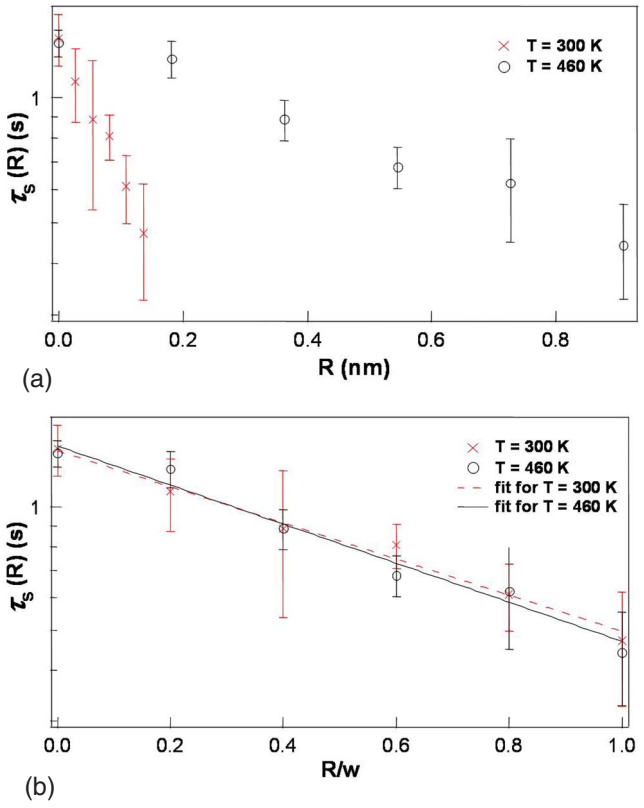

FIG. 6. (Color online) (a) The generalized survival time constants $\tau_s(R)$ vs R. The red crosses are $\tau_s(R)$ at 300 K and the black circles at 460 K. (b) The same data with R normalized by w. The red crosses are $\tau_s(R)$ at 300 K and the black circles at 460 K. The red dashed line and black solid line are corresponding unweighted exponential fits for these two data sets, respectively, $\tau_s(R) = \tau_{s0} \exp[-A(R/w)]$. The best fitting parameters are $\tau_{s0} = 1.37 \pm 0.03$ s, $A = 1.01 \pm 0.06$ for $\tau_s(R)$ at 300 K, and $\tau_{s0} = 1.40 \pm 0.06$ s, $A = 1.09 \pm 0.11$ for $\tau_s(R)$ at 460 K.

data show that the time constant is equal to $\tau_s(R) = \tau_{s0} \exp(-R/w)$ to well within one standard deviation. Even though the exponential dependence of the time constant on R is a phenomenological result of the simulation above and in Ref. [26], the above results confirm the observation and show that the offset value R should be scaled in terms of the step width in evaluating the generalized survival probability.

B. Generalized inside survival

The concept of generalized survival is related to a relaxation from a position outside the reference level to the reference level (e.g., it is related to one-sided statistics). Physically, and for possible applications, we also may be interested in another form of generalized survival, which is the probability for the step edge to remain between the preassigned reference positions R and $-R$ over a time interval t. In this case we are asking about the probability of the step, initially at a small displacement, not fluctuating to larger displacements. In order to distinguish this case from the generalized survival, we refer to it as the generalized inside survival $S_{\text{in}}(t,R)$. The definition is as follows:

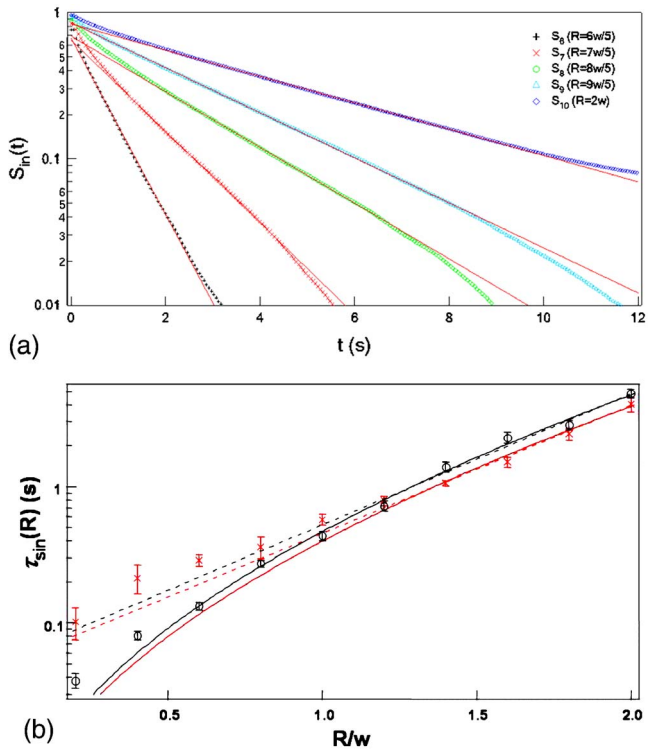

FIG. 7. (Color online) (a) The generalized inside survival probability curves $S_{\text{in}}(t,R)$ and corresponding fitting curves at 460 K. From lower to upper, the curves are respectively the generalized survival probability with respect to $R = 6w/5$, $7w/5$, $8w/5$, $9w/5$, and $2w$. The solid red lines are corresponding exponential fits for each curve. The time constants extracted from the fits are listed in Table I. (b) Time constants for the generalized inside survival probability $\tau_{\text{sin}}(R)$ vs R/w. The red crosses are $\tau_{\text{sin}}(R)$ at 300 K and the black circles at 460 K. The dashed lines are corresponding unweighted exponential fits for these two data sets, respectively, using the fitting formula $\tau_{\text{sin}}(R) = \tau_{\text{sin}\,0} \exp[A(R/w)^{\lambda}]$ with $\lambda = 1$. The best fitting values are $\tau_{\text{sin}\,0} = 0.05 \pm 0.01$ s, $A = 2.16 \pm 0.09$ for $\tau_{\text{sin}}(R)$ at 300 K (red), and $\tau_{\text{sin}\,0} = 0.06 \pm 0.01$ s, $A = 2.21 \pm 0.12$ for $\tau_{\text{sin}}(R)$ at 460 K (black). The solid lines are fits using the same fitting formula with $\lambda = 1/2$. The best fitting values are $\tau_{\text{sin}\,0} = 0.002 \pm 0.001$ s, $A = 5.50 \pm 0.39$ for $\tau_{\text{sin}}(R)$ at 300 K (red), and $\tau_{\text{sin}\,0} = 0.002 \pm 0.001$ s, $A = 5.58 \pm 0.30$ for $\tau_{\text{sin}}(R)$ at 460 K (black).

$$S_{\text{in}}(t,R) \equiv \text{Prob}\{-R < x(t') < R, \quad \forall\, t_0 \leqslant t' \leqslant t_0 + t\}. \tag{6}$$

The generalized inside survival probabilities also have a clear exponential behavior on time, as shown in Fig. 7(a). When R is less than w, the generalized survival decays quickly, with time constants less than 0.5 s. Given the sampling interval of 51.2 ms in our measurement, we obtain the most significant results with R values greater than w, although exponential decay is also clear at the smaller offsets. In contrast to the generalized survival, as R increases the generalized inside survival time constant also increases. This is reasonable intuitively, since it takes longer to cross larger or offsets because the average required step excursion is larger. Fitting these generalized inside survival experimental data yields characteristic time scales, the generalized inside

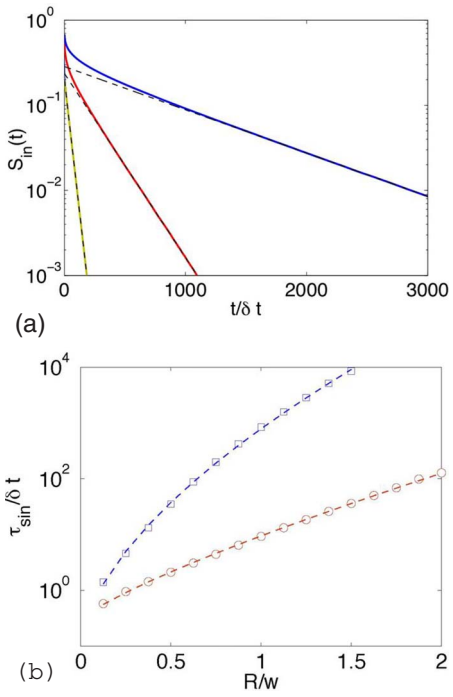

FIG. 8. (Color online) (a) The generalized inside survival probability $S_{in}(t,R)$ as a function of time t (scaled by the sampling interval $\delta t=1$) for three different values of the distance R. The thick lines [from top to bottom, $R/w=1.0$ (blue), 0.75 (red), and 0.5 (green)] represent the simulation data and the (black) dashed lines represent exponential fits to the long-time data. (b) Dependence of the time scale $\tau_{sin}(R)$, measured in units of the sampling interval δt, on the distance R, measured in units of the interface width w. In the upper curve of (b), the results obtained from equilibrium simulations for sample size $L=200$ and sampling interval $\delta t=1$ are shown by the (blue) squares. The (blue) dashed line passing through the data points represents a fit to the form $\tau_{sin}(R) \propto \exp[C_2(R/w)^{\lambda}]$ with $\lambda=0.59$. The lower curve in (b) shows the results [(red) circles] obtained from a "finite-time" simulation (see text) with measuring time $t_m=5000$ and $\delta t=2.5$. A fit of these data to the above form with $\lambda=0.8$ is shown by the (red) dashed line. The error bars for the simulation data are smaller than the size of the symbols used in the plots.

survival constants $\tau_{sin}(R)$, as shown in Fig. 7(b). The collapse of the curves with scaling as R/w is not as complete as for the generalized survival (Fig. 6), in particular with some deviation at 300 K for small R/w. The curves can be fit to an exponential form $\tau_{sin\,0} \exp[A(R/w)^{\lambda}]$, but the fits suggest a temperature dependence to the value of λ, as discussed below.

To determine the appropriate functional form for the dependence of the time constant on offset R, the inside survival probabilities were also determined from the numerical simulations, with results shown in Fig. 8 for three different values of R ($R/w=0.5$, 0.75, and 1.0). Fits of the long-time data to an exponential form are also shown to illustrate that the decay is exponential in time for large t. The data shown were obtained using $\delta t=1.0$. We have examined how the measured $S_{in}(t,R)$ depends on the values of the sampling time δt and the sample size L. These results are consistent with the scaling behavior found in Ref. [19] for the generalized survival probability:

$$S_{in}(t,R,\delta t,L) = f_1[t/\delta t, R/w(L), \delta t/\tau_c(L)], \tag{7}$$

where $w(L) \propto L^{1/2}$ is the equilibrium width and $\tau_c(L) \propto L^4$ is the correlation time of a step of length L, and f_1 is a scaling function.

The time scales $\tau_{sin}(R)$ associated with the exponential decay of $S_{in}(t,R)$ may be obtained from fits such as those shown in Fig. 8(a). The results of the numerical simulation for the dependence of τ_{sin} on R/w, obtained for $L=200$ and $\delta t=1$, are shown in the top plot in Fig. 8(b). It is clear from the plot that an exponential dependence, $\tau_{sin}(R) \propto \exp(C_2 R/w)$, does not provide a good description of the data: the plot of log τ_{sin} vs R/w clearly shows considerable curvature. Similar behavior was also found for the R dependence of τ_{sin} for the one-dimensional EW equation [31]. We have found that the empirical form $\tau_{sin}(R) \propto \exp[C_2(R/w)^{\lambda}]$, with C_2 a constant and $\lambda \approx 0.6$, provides a good description of the simulation data. A fit to this form with $\lambda=0.59$ is shown by the upper line in Fig. 8(b). For comparison, the experimental data in Fig. 7(b) are shown with curves for best fits to the pure exponential ($\lambda=1$) and exponential square root ($\lambda=1/2$) forms.

The results obtained from the equilibrium simulations described above are not directly comparable with those obtained from the experiments because in the experiments, the average step position is measured as an average over a finite measurement time t_m. This has been shown to be important [25], because measurements of the survival probabilities require knowledge of the true average step position: the quantity R is, by definition, the distance of the reference level from the true average step position. In simulations, the true average step position is known, as discussed above. In experiments, on the other hand, the average step position differs from the true position if t_m is less than τ_c because fluctuations with relaxation times larger than t_m cannot be thoroughly sampled during the measurement time. In experiments [25,29], the effect of using a finite t_m is approximately equivalent to that of having a finite system of size $L_{eff} \propto t_m^{1/n}$ with $n=4$ in the present case. This implies the following scaling dependence of the measured survival probability on the measurement time t_m:

$$S_{in}(t,R,\delta t,t_m) = f_2[t/\delta t, R/w(t_m), \delta t/t_m], \tag{8}$$

where $w(t_m)$ is the measured step width (i.e., the root-mean-square deviation of the step position from its apparent average value). In principle, the scaling function should also have as its argument another scaling variable t_m/τ_c. Note that this scaling form implies that if the measured $S_{in}(t,R)$ decays exponentially in time, then the time scale of this decay, measured in units of δt, should be a universal function of $R/w(t_m)$ if $\delta t/t_m$ is held fixed.

We have studied by simulation the effect of a finite measurement time on the behavior of the generalized inside survival probability. In these simulations, the Langevin equation was numerically integrated for time t_m, starting from an equilibrated step profile. The average $\bar{x}_i$ of $x_i(t)$ over the time

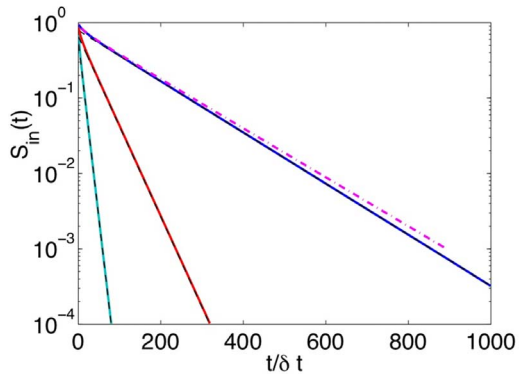

FIG. 9. (Color online) The generalized inside survival probability $S_{\rm in}(t,R)$, calculated from "finite-time" simulations with $t_m=5000$ and $\delta t=2.5$ (see text), as a function of time t scaled by the sampling interval δt, for three different values of the distance R. The thick lines [from top to bottom, $R/w=2.0$ (blue), 1.5 (red), and 1.0 (green)] represent the simulation data and the (black) dashed lines represent exponential fits to the long-time data. The (magenta) dash-dotted line shows the results for $R/w=2.0$ obtained from a simulation with $t_m=1000$ and $\delta t=0.5$.

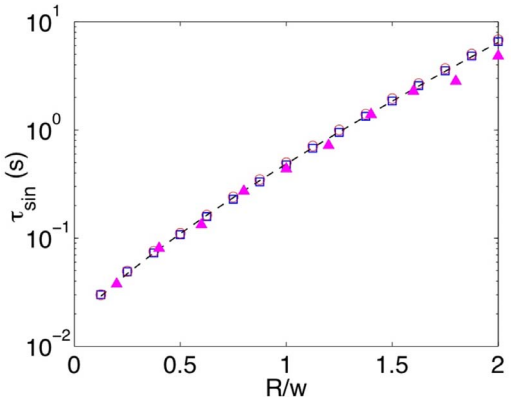

FIG. 10. (Color online) Comparison of numerical and experimental results for the time scale $\tau_{\rm sin}(R)$ of the decay of the generalized inside survival probability. The (blue) squares and (red) circles, respectively, represent the simulation results obtained for $t_m=5000$, $\delta t=2.5$ and for $t_m=1000$, $\delta t=0.5$. The experimental results for temperature $T=460$ K are shown by the (magenta) triangles. The (black) dashed line shows a fit of the simulation data to the empirical form, $\tau_{\rm sin}(R/w)\propto\exp[C_2(R/w)^{\lambda}]$, with $\lambda=0.8$.

period t_m was then taken to be the "experimentally measured" average step position at lattice site i, and the quantities $x_i'(t)\equiv x_i(t)-\bar{x}_i$ were used to define the interface width $w(t_m)$ and to calculate the generalized inside survival probability $S_{\rm in}(t,R)$ for different values of R (taken to be the distance from the "experimentally measured" average step position defined above). Our results for the dependence of the "experimentally measured" step width $w(t_m)$ on the measurement time t_m are in good agreement with those reported in Ref. [29]. In particular, we find that $w(t_m)\propto t_m^{1/2n}$ with $n=4$. Also, the numerically obtained distribution of the $x_i'(t)$ is very well described by a Gaussian with zero mean and width equal to $w(t_m)$, in further good agreement with the experimentally observed behavior of the distribution of the step displacements.

The results for the generalized inside survival probability with finite measurement time, obtained from the procedure described above, are shown in Fig. 9. The plots in this figure show results obtained from simulations with $t_m=5000$ and $\delta t=2.5$. It is clear from these plots that the "finite-time" $S_{\rm in}(t,R)$ decays exponentially in time for large t, and that the time scale $\tau_{\rm sin}$ of this decay increases with R. A plot for the time dependence of $S_{\rm in}(t,R)$ for $R/w=2.0$, obtained from simulations with $t_m=1000$ and $\delta t=0.5$, is also shown in the figure. Since $\delta t/t_m$ has the same value (=1/2000) in both the simulations, the scaling relation of Eq. (8) predicts that plots of $S_{\rm in}(t,R)$ vs $t/\delta t$ obtained from the two simulations with the same value of R/w should coincide. As shown in Fig. 9, the two plots are close to each other, but not exactly coincident. Thus, the scaling relation of Eq. (8) is approximately, but not exactly satisfied, probably reflecting a dependence on the additional scaling variable t_m/τ_c mentioned above. It is clear from the data that the time scale $\tau_{\rm sin}$ obtained from the simulation with $t_m=1000$ is slightly larger (by $\sim 5\%$) than the value obtained from the simulation with $t_m=5000$. A similar increase in $\tau_{\rm sin}$ with decreasing t_m is also found for other values of R/w and in simulations with smaller t_m.

The dependence of the time scale $\tau_{\rm sin}$ on R/w, obtained from the "finite-time" simulation with $t_m=5000$, $\delta t=2.5$, is shown in the bottom plot of Fig. 8(b). The empirical form $\tau_{\rm sin}(R)\propto\exp[C_2(R/w)^{\lambda}]$, provides a good description of the data, but with a value of λ (≈ 0.8) that is larger than that found for the results of the equilibrium simulation. A fit of the numerical results for $\tau_{\rm sin}$ to this form with $\lambda=0.8$ is also shown in Fig. 8(b). These results suggest that the value of λ is not "universal." It is also possible that this functional form does not represent the actual dependence of $\tau_{\rm sin}$ on R/w.

The values of t_m and δt in the "finite-time" simulations were chosen so as to make the value of the scaling variable $\delta t/t_m$ the same as that (1/2000) used in the experiments. If the scaling relation of Eq. (8) is valid (as discussed above, our simulation results indicate that it is valid to a good approximation), then the results for $\tau_{\rm sin}/\delta t$ obtained from simulations should match those obtained in the experiment for the same value of R/w. To test this prediction, we have multiplied the simulation results for $\tau_{\rm sin}/\delta t$ by the δt (0.0512 s) used in the experiment to obtain values of $\tau_{\rm sin}(R/w)$ in physical time units (seconds) for different R/w. Figure 10 shows a comparison of the values of $\tau_{\rm sin}$ obtained this way with the experimental results obtained at temperature $T=460$ K. It is clear from the plots in this figure that the simulation results are in good agreement with the experimental ones. The small differences between the two sets of results for R/w near 2.0 may be due to insufficient sampling of the tails of the Gaussian distribution of the step displacement in the experiment.

Since the experimental measurements at temperatures 460 and 300 K were carried out with the same values of t_m and δt, the scaling behavior discussed above suggests that the values of $\tau_{\rm sin}$ for these two temperatures should be the same for a fixed R/w. As shown earlier [Fig. 7(b)], the experimental results for $\tau_{\rm sin}$ at $T=300$ K do not collapse to the same shape as those at 460 K when scaled as R/w. The experimental data were carefully evaluated, and there is no appar-

ent systematic problem that could explain this difference. However, an underlying physical cause may arise from a dependence of the scaling function in Eq. (8) on the additional scaling variable $t_m/\tau_{c,\mathrm{true}}$. The expected temperature dependence of the physical parameters that govern the step fluctuations indicates that the true correlation time $\tau_{c,\mathrm{true}}$ increases by three orders of magnitude as T is decreased from 460 to 300 K. Since t_m is the same at the two temperatures, the corresponding values of $t_m/\tau_{c,\mathrm{true}}$ would also differ by three orders of magnitude. The experimental offset in the values of τ_{sin} measured at the two temperatures is consistent with the direction of offset shown in Fig. 9. The question of whether the more dramatic change of the experimental $\tau_{c,\mathrm{true}}$ might also account for the apparent change in the fit parameter λ, unfortunately, cannot be immediately tested numerically because t_m can not be changed by several orders of magnitude in the simulation.

IV. DISCUSSION

The first discussions of survival probability focused on the question of one-sided crossing of the average position ($x=0$) of the step. This probability is related to the experimental problem of the time for relaxation of a step initially displaced by a distance x_0 from equilibrium, which is expected to go as [33,36,37]

$$\langle x\rangle = x_0 \exp(-t/\tau_{\mathrm{eq}}), \tag{9}$$

where τ_{eq} has been shown to equal the correlation time τ_c, for the cases of attachment and detachment and periphery diffusion limited step fluctuations. The relationship of the survival time constant to the correlation time is thus intuitively reasonable. Here we have tested the numerical prediction for a broader definition of survival (generalized survival) involving one-sided crossing of a boundary displaced by an offset R from the average step position. The maximum survival probability $[S(0)]$ in this case reduces to the probability of initially finding the step at a displacement greater than R:

$$S(0,R) = \int_{|x|>R} \frac{1}{w\sqrt{2\pi}} \exp(-x^2/2w^2)dx. \tag{10}$$

As shown in Table I and Fig. 4, the experimental values of $S(0,R)$ agree with the known values of Eq. (10).

As predicted theoretically, our generalized survival data are well fitted to a functional form

$$S(t,R) = S_0 \exp[-t/\tau_s(R)]. \tag{11}$$

In addition, we show empirically that the offset-dependent time constant $\tau_s(R)$ also follow a simple relationship

$$\tau_s(R) = \tau_{s0} \exp(-R/w). \tag{12}$$

This is consistent with numerical results that showed the exponential dependence of the time constant on the offset distance R. It is also consistent with the theoretical scaling form of the generalized survival probability [26]

TABLE II. Experimental parameters for the inside survival for offset values ranging from $R=1.2w$ to $R=2w$. The expected values for $S_{\mathrm{in}}(0)$ based on the Gaussian distribution are 0.770 ($R/w=1.2$), 0.838 ($R/w=1.4$), 0.890 ($R/w=1.6$), 0.928 ($R/w=1.8$), and 0.954 ($R/w=2.0$).

T (K)	R/w	$S_{\mathrm{in}}(0)$	$\tau_{\mathrm{in}}(R)$
300	1.2	0.77±0.02	0.79±0.06
	1.4	0.84±0.01	1.06±0.05
	1.6	0.89±0.01	1.51±0.13
	1.8	0.93±0.01	2.44±0.24
	2.0	0.96±0.01	4.04±0.50
460	1.2	0.76±0.01	0.72±0.06
	1.4	0.84±0.01	1.39±0.12
	1.6	0.89±0.01	2.28±0.21
	1.8	0.930±0.004	2.83±0.21
	2.0	0.956±0.005	4.83±0.34

$$S(t,L,R,\delta t) = f\left(\frac{t}{L^4}, \frac{R}{L^a}, \frac{\delta t}{L^4}\right), \tag{13}$$

where L is the system size and α is the roughness exponent, which for steps on Ag(111) surfaces in this temperature range, is 1/2 [38]. The relationship between w and L [see Eq. (3)] is $w \propto L^{1/2}$. Thus our observed scaling form with R/w as the scaling variable is consistent with the theoretical prediction of R/L^{α} scaling at any fixed temperature. For physical systems, the identification of the step width as the relevant variable that sets the scale of the offset distance R further allows quantitative prediction of the variation of the survival time constant with changing physical parameters such as temperature, step stiffness and step mobility.

The generalized inside survival probability physically provides complementary information to the generalized survival. As expected, the values at $t=0$, shown in Tables I and II, reflect the Gaussian distribution of Fig. 4 and Eq. (10), yielding $S_{\mathrm{in}}(0,R)=1-S(0,R)$. The exponentially increasing time constants for the inside survival, as the offset distance R increases, reflect physically the effect of the restoring force (due to the step stiffness) opposing the outward displacement of the step that would allow it to cross the offset position.

For both generalized probabilities considered, the dependence of the relaxation time constant on offset has not been determined analytically. The problem is especially difficult for inside survival, which does not have the clear relationship to the problem of one-sided statistics that has been used to evaluate generalized survival. Our results, both numerical and experimental, however, provide clear evidence for a functional form $\tau_{\mathrm{sin}\,0} \exp[A(R/w)^{\lambda}]$, that must be numerically equivalent to any analytical solution in the parameter space accessible to the experiments and simulations.

For applications, both the generalized survival and the generalized inside survival provide an approach for evaluating the impact of stochastic behavior on future nanometer scale electronic devices. The results here show that this can be accomplished semiquantitatively given only knowledge of

the measurement time and the interface width. For instance, we can consider the combination of the two generalized survival probabilities $1-S(R,t)-S_{\mathrm{in}}(R,t)=P_c(R,t)$, where $P_c(R,t)$ is the probability that the step edge does cross the preassigned reference positions R $(-R)$ for any given starting point. Such a problem may be related to a specific behavior that would be triggered by first arrival at the reference point. At present, the effects of atomic-scale structural variation on interconnections in nanoelectronics and molecular electronics are in the early stages of understanding [39,40]. As our ability to control interfaces grows, it may be possible to exploit such quantitative statistical knowledge of the effects of thermal fluctuations.

ACKNOWLEDGMENTS

This work has been supported by the UMD NSF-MRSEC under Grant No. DMR 05-20471, and the MRSEC-SEF, and by the IIT. The authors thank M. Constantin and S. Das Sarma for encouragement in this work.

[1] V. V. Zhirnov and R. K. Cavin, Nat. Mater. **5**, 11 (2006).
[2] G. K. Ramachandran, T. J. Hopson, A. M. Rawlett, L. A. Nagahara, A. Primak, and S. M. Lindsay, Science **300**, 1413 (2003).
[3] B. Q. Xu and N. J. J. Tao, Science **301**, 1221 (2003).
[4] W. Y. Wang, T. H. Lee, and M. A. Reed, Proc. IEEE **93**, 1815 (2005).
[5] S. H. Ke, H. U. Baranger, and W. T. Yang, J. Chem. Phys. **123**, 114701 (2005).
[6] M. Giesen, Prog. Surf. Sci. **68**, 1 (2001).
[7] H. C. Jeong and E. D. Williams, Surf. Sci. Rep. **34**, 175 (1999).
[8] M. J. Rost, S. B. van Albada, and J. W. M. Frenken, Phys. Rev. Lett. **86**, 5938 (2001).
[9] S. Kodambaka, V. Petrova, S. V. Khare, D. D. Johnson, I. Petrov, and J. E. Greene, Phys. Rev. Lett. **88**, 146101 (2002).
[10] E. Le Goff, L. Barbier, and B. Salanon, Surf. Sci. **531**, 337 (2003).
[11] M. Ondrejcek, M. Rajappan, W. Swiech, and C. P. Flynn, Phys. Rev. B **73**, 035418 (2006).
[12] S. Redner, *A Guide to First-Passage Processes* (Cambridge University Press, Cambridge, 2001).
[13] J. Merikoski, J. Maunuksela, M. Myllys, J. Timonen, and M. J. Alava, Phys. Rev. Lett. **90**, 024501 (2003).
[14] V. B. P. Leite, L. C. P. Alonso, M. Newton, and J. Wang, Phys. Rev. Lett. **95**, 118301 (2005).
[15] I. Goychuk and P. Hanggi, Proc. Natl. Acad. Sci. U.S.A. **99**, 3552 (2002).
[16] J. Z. Y. Chen, H. K. Tsao, and Y. J. Sheng, Phys. Rev. E **72**, 031804 (2005).
[17] J. Krug, Physica A **340**, 647 (2004).
[18] M. Constantin, C. Dasgupta, P. Punyindu Chatraphorn, S. N. Majumdar, and S. Das Sarma, Phys. Rev. E **69**, 061608 (2004).
[19] M. Constantin and S. Das Sarma, Phys. Rev. E **70**, 041602 (2004).
[20] D. B. Dougherty, O. Bondarchuk, M. Degawa, and E. D. Williams, Surf. Sci. **527**, L213 (2003).
[21] M. Constantin, S. Das Sarma, C. Dasgupta, O. Bondarchuk, D. B. Dougherty, and E. D. Williams, Phys. Rev. Lett. **91**, 086103 (2003).
[22] D. B. Dougherty, I. Lyubinetsky, E. D. Williams, M. Constantin, C. Dasgupta, and S. Das Sarma, Phys. Rev. Lett. **89**, 136102 (2002).
[23] J. Krug, H. Kallabis, S. N. Majumdar, S. J. Cornell, A. J. Bray, and C. Sire, Phys. Rev. E **56**, 2702 (1997).
[24] M. Constantin, S. Das Sarma, and C. Dasgupta, Phys. Rev. E **69**, 051603 (2004).
[25] D. B. Dougherty, C. Tao, O. Bondarchuk, W. G. Cullen, E. D. Williams, M. Constantin, C. Dasgupta, and S. Das Sarma, Phys. Rev. E **71**, 021602 (2005).
[26] M. Constantin and S. Das Sarma, Phys. Rev. E **69**, 052601 (2004).
[27] A. A. Baski and H. Fuchs, Surf. Sci. **313**, 275 (1994).
[28] M. Levlin and A. Laakso, Appl. Surf. Sci. **171**, 257 (2001).
[29] O. Bondarchuk, D. B. Dougherty, M. Degawa, E. D. Williams, M. Constantin, C. Dasgupta, and S. Das Sarma, Phys. Rev. B **71**, 045426 (2005).
[30] F. Mugele, A. Rettenberger, J. Boneberg, and P. Leiderer, Surf. Sci. **400**, 80 (1998).
[31] C. Dasgupta (unpublished).
[32] C. Tao, T. J. Stasevich, T. L. Einstein, and E. D. Williams, Phys. Rev. B **73**, 125436 (2006).
[33] N. C. Bartelt, J. L. Goldberg, T. L. Einstein, and E. D. Williams, Surf. Sci. **273**, 252 (1992).
[34] S. N. Majumdar and C. Dasgupta, Phys. Rev. E **73**, 011602 (2006).
[35] C. Dasgupta, M. Constantin, S. Das Sarma, and S. N. Majumdar, Phys. Rev. E **69**, 022101 (2004).
[36] M. B. Webb, F. K. Men, B. S. Swartzentruber, R. Kariotis, and M. G. Lagally, Surf. Sci. **242**, 23 (1991).
[37] F. K. Men, W. E. Packard, and M. B. Webb, Phys. Rev. Lett. **61**, 2469 (1988).
[38] A.-L. Barabasi and H. E. Stanley, *Fractal Concepts in Surface Growth* (Cambridge University Press, Cambridge, 1995).
[39] H. Basch, R. Cohen, and M. A. Ratner, Nano Lett. **5**, 1668 (2005).
[40] C. Tao, T. J. Stasevich, W. G. Cullen, T. L. Einstein, and E. D. Williams, Nano Lett. **7**, 1495 (2007).